Indian Journal of Pure & Applied Physics
Vol. 59, October 2021, pp. 700-705

A Facile Method of Synthesis and Characterization of Sr Doped CeO_2 Nanocrystalline Materials

G Gnanasangeetha[a*], V Asvini[b], G Karthik[b] & K Ravichandran[b]

[a]Department of Theoretical Physics, University of Madras, Guindy Campus, Chennai – 600 025, India

[b]Department of Nuclear Physics, University of Madras, Guindy Campus, Chennai – 600 025, India

Received 21 December 2019; accepted 26 September 2021

Strontium doped Cerium oxide ($Ce_{1-0.25}Sr_{0.25}O_2$ and $Ce_{1-0.5}Sr_{0.5}O_2$) nanocrystals were synthesized by combustion technique. The synthesized ($Ce_{1-x}Sr_xO_2$, x = 0.25, 0.5) nanocrystals were annealed at 500° C for 2hr. The phase formation, surface morphology and elemental composition analysis have been studied using XRD, HRSEM and EDXS. XRD and HRSEM measurements revealed that the synthesized nanocrystals were in single phase with face-centered cubic (fcc) structure and that the nano-grains had different sizes. Chemical composition was confirmed using EDXS. The UV-Vis spectroscopic studies revealed that as the Sr doping level increases, the band gap width increases from E_g = 2.9 eV to 2.95 eV. At the same time, the wavelength of maximum absorbance shifts from λ_{abs} = 285 to 300 nm. Further, PL studies were performed with excitation wavelength λ = 350 nm and two main emission peaks were observed at 415 and 437 nm respectively. TGA, DTA and DSC measurements were carried out to check the weight loss and the occurrence of endothermic/exothermic reactions.

Keywords: Cerium oxide, Strontium metal, Combustion, XRD, HRSEM, EDX, UV, PL, TGA/DTA and DSC.

1 Introduction

Cerium (Ce), a rare earth metal belonging to the lanthanide series and one of the most abundant element in nature, exists in one of the two oxidation (reduced and oxidized) states: either cerous (Ce^{3+}, trivalent state) or ceric (Ce^{4+}, tetravalent state) [1]. It is a ductile and malleable lustrous metal, which is iron-gray in color and highly reactive. Ceria (CeO_2) is a metal oxide n-type semiconductor[2], that has band gap energy E_g = 3-3.6 eV, high dielectric constant κ = 23–26, refractive index n: 2.2 – 2.8 and high dielectric strength up to 2.6 MV cm^{-1}. Cerium oxide (CeO_2) has exceptional technological importance due to its unique properties; particularly it behaves as a very good oxide-ion conductor in the case of solid oxide fuel cells and has excellent oxygen storage capacity, due to its high oxygen deficiency[3-5]. It is also used as an ultraviolet absorber [6-7], finds applications in gas sensors [8-13] while nanoceria plays a major role in cosmetic products as UV blockers [14].

In the recent years, doped CeO_2 has been an attractive candidate for both technological applications as well as scientific research. Various conventional techniques are available for the synthesis of Srontium (Sr) doped CeO_2 nano-powders such as sol-gel[15], hydrothermal[16], thermal decomposition[17], and combustion[18]. Among the various methods, the combustion technique is not only easier to handle but also efficient. Further, it is cost-effective and requires less effort to produce the ultrafine powder of Sr doped CeO_2 with narrow size distribution. In this work, nano-sized Sr doped Ceria ($Ce_{(1-x)}Sr_xO_2$, where x = 0.25, 0.5) have been synthesized by the combustion technique. We have characterized these samples and studied in detail the effect of doping CeO_2 with Sr. The results show that there is an enhancement of structural, optical, and thermal properties due to change in the dopant concentration.

2 Experimental Details

Commercially available powders of Cerium Nitrate [$Ce(NO_3)_3.6H_2O$], Urea [$(NH_2)_2Co$], Succinic acid [$C_4H_6O_4$], Strontium nitrate [$Sr(NO_3)_2$] (AR grade, Sigma Aldrich, USA, 99.9% purity) were used as starting materials. After synthesis, the doped samples $Ce_{1-0.25}Sr_{0.25}O_2$ and $Ce_{1-0.5}Sr_{0.5}O_2$ were annealed at a temperature of 500° C for 2 hr. XRD measurements were carried out for both the undoped and doped samples, using Bruker D8 Advance diffractometer with $Cu_{K\alpha}$ radiation (λ = 1.5406 Å) as

*Corresponding author (E-mail: sangee@unom.ac.in)

the radiation source, Ni filter and operating voltage of 40 kV at the current of 35 mA. The two doped samples were subjected to additional characterizations. Surface morphology and elemental analysis were studied using high resolution scanning electron microscopy and energy dispersive x-ray analysis (HRSEM with EDXS: Hitachi-S4800) at an operating voltage of 15kV. The UV spectra were measured with UV-Vis spectrophotometer (Shimadzu UV-2600) and the absorption spectrum was recorded in the wavelength range λ = 200 to 900 nm. The band gap energy was obtained by Kubelka-Munk function versus energy. The Photoluminescence (PL) measurement was carried out using HORIBA (FL3C-21-1962C-1318-FL) system with excitation wavelength λ = 350 nm. Thermal studies were carried out using simultaneous Thermogravimetric/Differential Thermal Analysis (TG/DTA), and Differential Scanning Calorimetry (DSC) in N_2 atmosphere at a heating rate of 10°C/ minute. The recorded range of temperature profiles was calibrated with standard calibration materials (Nickel or iron, calcium (II) oxalate monohydrate $CaC_2O_4.H_2O$, silver and gold).

3 Results and Discussion

3.1 X-Ray Diffraction Studies

Fig.1 shows the powder X-ray diffraction ($Cu_{k\alpha}$, λ = 1.5406 Å) of Sr doped CeO_2 sample. Fig.1(a) shows the peaks of undoped CeO_2. In comparison Fig. 1(b) shows that the doped sample $Ce_{1-0.25}Sr_{0.25}O_2$ exhibits better defined peaks, *i.e.* higher crystalline quality after annealing. The diffraction peaks are indexed as (111), (200), (220), (311), (222), (400)* and (331)* corresponding to the diffraction angle 2θ = 28.45°, 32.94°, 47.32°, 56.12°, 58.84°, 69.02°, and 76.49°, respectively. Stars indicate the presence of Sr peaks in the Cerium oxide matrix. It was noted that Sr addition actually increases the crystalline quality of the nano-powders, in particular for the Sr fraction 0.25 whereas with the fraction 0.50 the FWHM (full width at half maximum) of all significant peaks seems larger as seen in Fig 1(c).

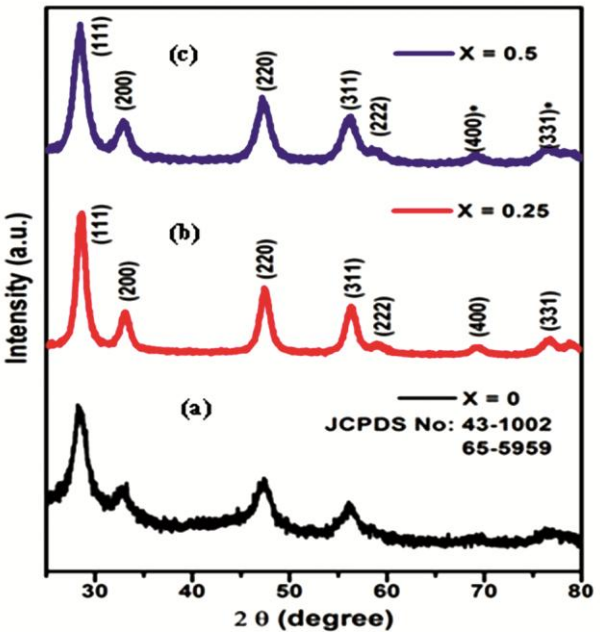

Fig.1 — X-ray diffraction plots of Sr doped CeO_2 (a) $Ce_{(1-x)}Sr_xO_2$ (x=0) (b) $Ce_{(1-x)}Sr_xO_2$ (x = 0.25) annealed at 500° C for 2 hr, (c) $Ce_{(1-x)}Sr_xO_2$, (x = 0.5) annealed at 500° C for 2 hr.

The XRD patterns confirm the $Fm\bar{3}m$ space group, face-centered cubic structure with cell parameter (*a* = 5.43 Å ± 0.0115) and volume =160.049 $Å^3$. The average crystallite size was calculated by Scherrer's formula (JCPDS # 43-1002 for pure CeO_2, 65-5959 for Sr). The average crystallite size was found to be 2.63 nm for pure CeO_2 and 4.78 nm for the doped sample $Ce_{1-0.25}Sr_{0.25}O_2$. The $Ce_{1-0.5}Sr_{0.5}O_2$ doped sample on the other hand confirms the face-centered cubic structure but the average crystallite size was found to be 5.85 nm. Thus, one can conclude that increasing the dopant concentration increases the crystallite size with respect to that of pure Ceria.

3.2 HRSEM Spectroscopy

HRSEM morphology of Sr doped CeO_2 nanoparticles annealed at 500° C for 2 hr is shown in Fig. 2(a) $Ce_{1-0.25}Sr_{0.25}O_2$ and (b) $Ce_{1-0.5}Sr_{0.5}O_2$. It is observed that particles with porous nature as well as agglomerates are bonded together. The agglomeration was found to increase with increasing Sr doping of the CeO_2 samples.

3.3 EDXS Studies

The EDX spectra of the doped samples $Ce_{1-0.25}Sr_{0.25}O_2$, and $Ce_{1-0.5}Sr_{0.5}O_2$ are shown in Figs. 3(a) and 3(b) respectively. The spectra clearly show the presence of the elements Sr, Ce and O, thus confirming the chemical composition of the powders.

3.4 UV-Visible Studies

Optical (UV-Visible) absorption spectra of Sr doped CeO_2 samples are shown in Fig. 4. For the samples $Ce_{1-0.25}Sr_{0.25}O_2$ and $Ce_{1-0.5}Sr_{0.5}O_2$, maximum absorption is found to occur at wavelengths λ = 285 nm and λ = 300 nm, respectively. The strong absorption peaks below 500 nm in the spectrum, is due to the charge transfer from O (2p) to Ce (4f) states in CeO_2

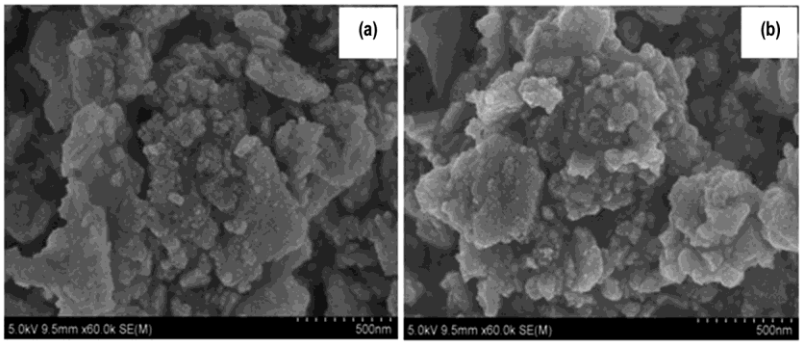

Fig. 2 — SEM images of Sr doped CeO_2: (a) $Ce_{1-0.25}Sr_{0.25}O_2$ and (b) $Ce_{1-0.5}Sr_{0.5}O_2$.

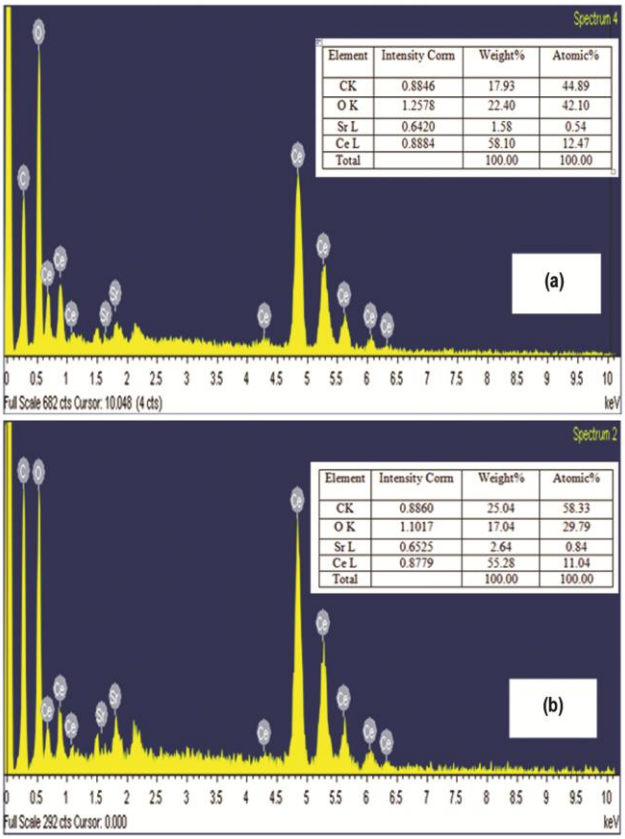

Fig. 3 — EDX spectra of Sr doped CeO_2 nanoparticles: (a) $Ce_{1-0.25}Sr_{0.25}O_2$, and (b) $Ce_{1-0.5}Sr_{0.5}O_2$ samples.

sample. The optical band gap was calculated from the Tauc plot of the Sr doped CeO_2 using the equation:

$$E_g = \frac{1240}{\lambda_{Absorp\ .Edge}}$$

Due to the increase in the Sr dopant in CeO_2, the optical properties also changes. That is, increase in Sr concentration in CeO_2 results in wider bandgap as well as increase of the wavelength at the maximum absorption. The band gap energies of $Ce_{1-0.25}Sr_{0.25}O_2$, and $Ce_{1-0.5}Sr_{0.5}O_2$ samples were calculated to be

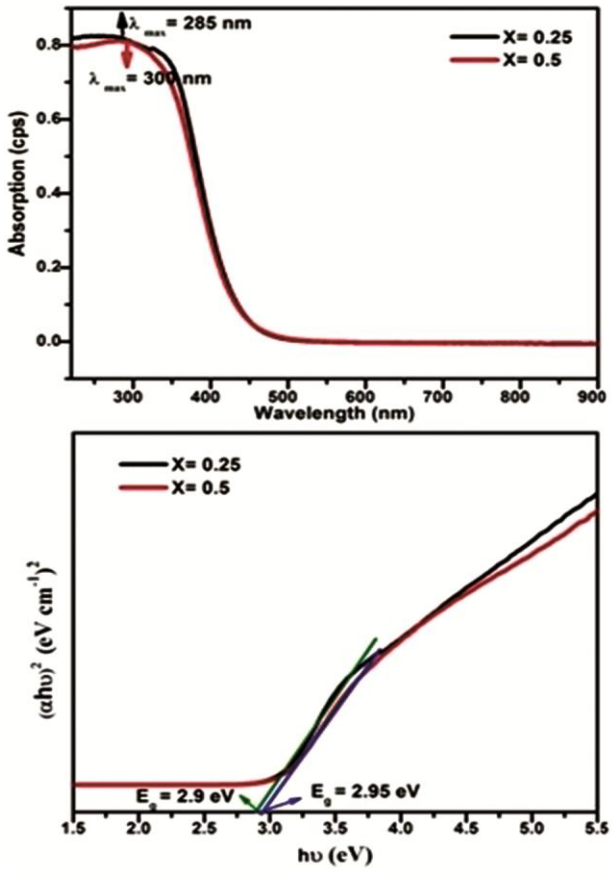

Fig. 4 — Shows the optical absorption and optical band gap energy of $Ce_{1-0.25}Sr_{0.25}O_2$ and $Ce_{1-0.5}Sr_{0.5}O_2$ samples by Tauc plot.

E_g = 2.9 eV and E_g = 2.95 eV respectively, using the Kubelka-Munk formula.

3.5 Photoluminescence

The photoluminescence of Sr doped CeO_2 ($Ce_{1-0.25}Sr_{0.25}O_2$ and $Ce_{1-0.5}Sr_{0.5}O_2$) nanoparticles was recorded at room temperature using Xenon lamp with excitation wavelength ($\lambda_{excitation}$ = 350 nm). A broad emission from 400 to 500 nm was observed,

presenting two distinct features at 415 nm and 437 nm as seen in Fig. 5. In the case of Sr doped ceria $Ce_{1-0.25}Sr_{0.25}O_2$, the emission intensity of the peak around 415 nm was found to slightly shift towards higher wavelength upon Sr doping, which suggests the existence of a large amount of oxygen vacancies.

These oxygen vacancies facilitate the charge transfer or hopping between the Ce (4f) level and the O (2p) level (valence band). This also indicates that the surface defects increased due to the Sr doping.

3.6 Thermogravimetric Analysis (TGA)

Thermal analysis (TGA, DSC and DTA) is a group of techniques in which the physical/chemical properties of a substance and/or its reaction products are measured as a function of temperature, by subjecting the substance to a gradual temperature variation. Among these techniques, TGA was used to determine thermal stability (quantitative weight loss or decomposition) of the prepared $Ce_{1-0.25}Sr_{0.25}O_2$, and $Ce_{1-0.5}Sr_{0.5}O_2$ materials.

Fig. 6(a) shows two noticeable changes, first, in the temperature range from 50° C to 125° C, an initial weight loss (1.47%) was observed due to the evaporation of adsorbed water molecules and, second, in the temperature range from 125° C to 1000°C major weight loss (1.71%) was obtained, which is due to decomposition of residual organic moieties present in Sr doped CeO_2, ($Ce_{1-0.25}Sr_{0.25}O_2$) sample. The total weight loss was thus found to be 3.18% for $Ce_{1-0.25}Sr_{0.25}O_2$ and 6.43 % for $Ce_{1-0.5}Sr_{0.5}O_2$ as shown in Figs 6(a) and (b) respectively.

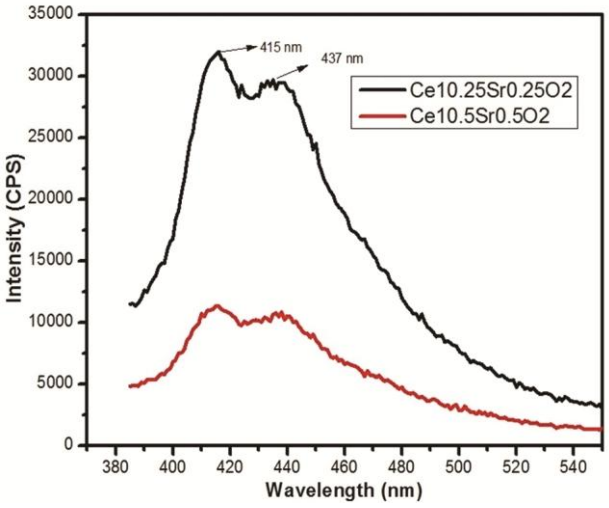

Fig. 5 — Photoluminescence spectrum of nanocrystalline $Ce_{1-0.25}Sr_{0.25}O_2$, (black color) and $Ce_{1-0.5}Sr_{0.5}O_2$ (red color) samples.

3.7 DSC Studies

DSC is used to measure the amount of energy or power absorbed (endothermic) or released (exothermic) by the sample as it is heated/cooled or held at a constant temperature. In this study, the DSC curve appears as a single endothermic peak around 160.9° C for $Ce_{1-0.25}Sr_{0.25}O_2$ and 163.9° C for $Ce_{1-0.5}Sr_{0.5}O_2$ samples, which indicates an increase in enthalpy, however, it is yet to be understood if it involves a phase transition. (Fig.7).

3.8 DTA Studies

DTA measures the difference in temperature between the sample and reference material when both are heated/cooled at a uniform rate. This analysis was used to determine the endothermic or exothermic reactions of the prepared $Ce_{1-0.25}Sr_{0.25}O_2$, and $Ce_{1-0.5}Sr_{0.5}O_2$ materials and is shown in Fig. 8.

The DTA results show that an endothermic peak appeared around 125° C due to evaporation of water. The predominant exothermic peak around 800° C was obtained, due to decomposition of residual organic moieties present in Sr doped CeO_2.

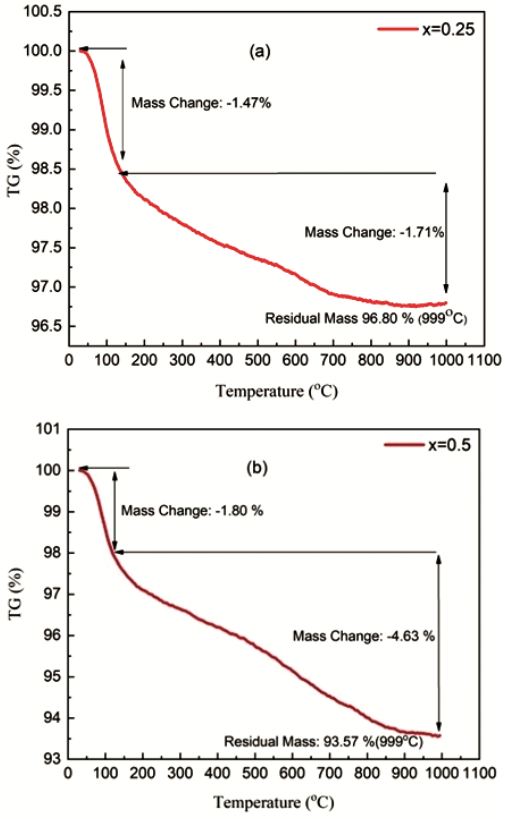

Fig. 6 — Thermogravimetric analysis of (a) $Ce_{1-0.25}Sr_{0.25}O_2$ and (b) $Ce_{1-0.5}Sr_{0.5}O_2$ annealed at 500° C for 2h.

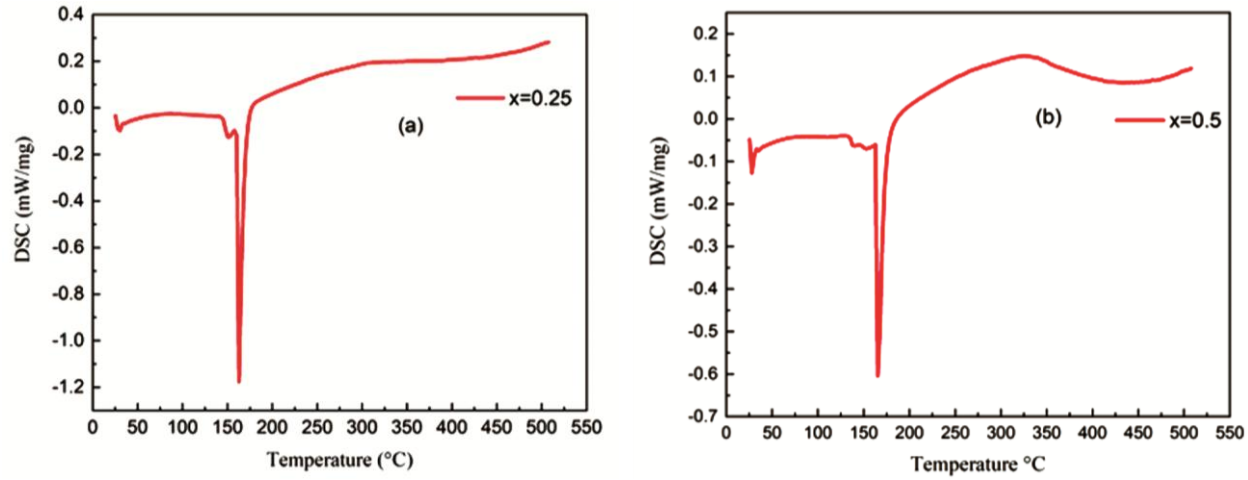

Fig. 7 — Differential scanning calorimetry of (a) $Ce_{1-0.25}Sr_{0.25}O_2$ and (b) $Ce_{1-0.5}Sr_{0.5}O_2$ at 500° C annealed for 2h.

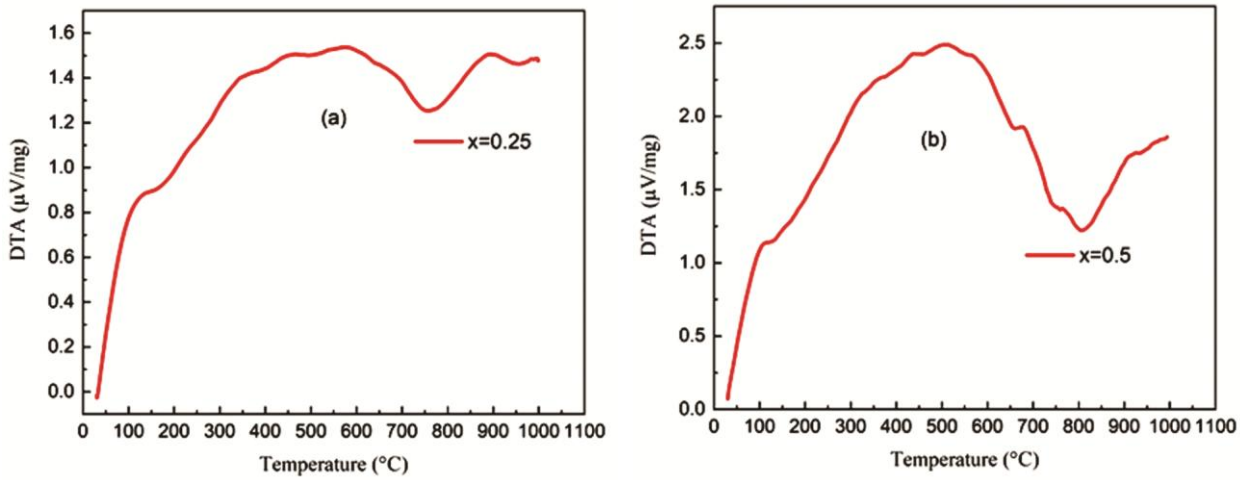

Fig. 8 — Differential thermal analysis of (a) $Ce_{1-0.25}Sr_{0.25}O_2$ and (b) $Ce_{1-0.5}Sr_{0.5}O_2$ at 500° C annealed for 2h.

4. Conclusions

In this work, Sr doped CeO_2 nanocrystals, with Sr fractions of 0.25 and 0.50 were successfully synthesized by the combustion technique. After annealing at 500 °C the samples became crystalline and exhibited face-centered cubic structure as confirmed by XRD measurements.

The surface morphology and elemental compositional analysis was carried out by HRSEM and EDX on doped samples with different Sr content. The UV-Vis and PL measurements confirmed that as the Sr concentration increases in CeO_2, the absorption peaks and band gap energy also shift to higher wavelength and higher energy respectively. The thermal analysis revealed that upon increase in the temperature, weight loss and endothermic or exothermic peaks were obtained.

Acknowledgement

The authors G. Gnanasangeetha and K. Ravichandran would like to thank the Department of Chemistry, IIT Madras, Chennai for the XRD measurements.

References

1 Korsvik C, Patil S, Seal S & Self W T, *Chem Commun*, 10 (2007) 1056.
2 Vangelista S, Piagge R, Ek S, Sarnet T, Ghidini G, Martella C & Lamperti A, *Thin Solid Films*, 636 (2017) 78.
3 Devaraju M K, Yin S & Sato T, *ACS Appl Mater Interfaces*, 1 (2009) 2694.
4 Djuricic B & Pickering S, *J Eur Ceram Soc*, 19 (1999) 1925.
5 Kamruddin M, Ajikumar P K, Nithya R, Tyagi A K & Raj B, *Scr Mater*, 50 (2004) 417.
6 Hernandes-Alonso M D, Hungria A B, Martinez- Arias A, Coronado J M, Conesa J C, Soria J & Fernandez-Garcia M, *Phys Chem Chem Phys*, 6 (2004) 3524.

7 Dao N N, Luu M D, Nguyen Q K & Kim B S, *Adv Nat Sci Nanosci Nanotechnol*, 2 (2011) 045013.

8 Zholobak N M, Ivanov V K, Shcherbakov A B, Shaporev A S, Polezhaeva O S, Baranchikov A Y, Spivak N Y, Tretyakov Y D, *J Photochem Photobiol B*, 102 (2011) 32.

9 Courbiere B, Auffan M, Rollais R., Tassistro V, Bonnefoy A, Botta A, Rose J, Orsiere T & Perrin J, *Int J Mol Sci*, 14 (2013) 21613.

10 De Marzi L, Monaco A, De Lapuente J, Ramos D, Borras M, Di Gioacchino M, Santucci S & Poma A, *Int J Mol Sci*, 14 (2013) 3065.

11 Demokritou P, Gass S, Pyrgiotakis G, Cohen J M, Goldsmith W, McKinney W, Frazer D, Ma J, Schwegler-Berry D, Brain J, & Castranova V, *Nanotoxicology* ,7 (2013) 1338.

12 Peng L, He X, Zhang P, Zhang J, Li Y, Zhang J, Ma Y, Ding Y, Wu Z, Chai Z & Zhang Z, *Int J Mol Sci*, 15 (2014) 6072.

13 Pulido-Reyes G, Rodea-Palomares I, Das S, Sakthivel T S, Leganes F, Rosal R, Seal S & Fernandez-Pinas F, *Sci Rep*, 5 (2015) 15613.

14 Zhang Y-W, Si R, Liao C-S, Yan, C-H, Xiao C-X & Kou Y, *J Phys Chem B*, 107 (2003) 10159.

15 Tambat S, Umale S & Sontakke S, *Mater Res Bull*, 76 (2016) 466.

16 Deus R C, Cortes J A, Ramirez M A, Ponce M A, Andres J, Rocha L S R, Longo E & Simoes A Z, *Mater Res Bull*, 70 (2015) 416.

17 Sharma J K, Srivastava P, Ameen S, Akhtar M S, Sengupta S K & Singh G, *Mater Res Bull*, 91 (2017) 98.

18 Umale S V, Tambat S N & Sontakke S M, *Mater Res Bull*, 94 (2017) 483.